blood®
Regular Article

THROMBOSIS AND HEMOSTASIS

Identification of the integrin-binding site on coagulation factor VIIa required for proangiogenic PAR2 signaling

Andrea S. Rothmeier,[1] Enbo Liu,[2] Sagarika Chakrabarty,[1] Jennifer Disse,[1] Barbara M. Mueller,[2] Henrik Østergaard,[3] and Wolfram Ruf[1,4]

[1]Department of Immunology and Microbiology, The Scripps Research Institute, La Jolla, CA; [2]San Diego Biomedical Research Institute, San Diego, CA; [3]Novo Nordisk A/S, Maløv, Denmark; and [4]Center for Thrombosis and Hemostasis, Johannes Gutenberg University Medical Center, Mainz, Germany

KEY POINTS

- The FVIIa integrin-binding motif is required for TF-FVIIa complex formation with integrin β1 and proangiogenic signaling.
- The arf6 integrin recycling pathway controls TF-FVIIa signaling and cell surface availability for procoagulant activity.

The tissue factor (TF) pathway serves both hemostasis and cell signaling, but how cells control these divergent functions of TF remains incompletely understood. TF is the receptor and scaffold of coagulation proteases cleaving protease-activated receptor 2 (PAR2) that plays pivotal roles in angiogenesis and tumor development. Here we demonstrate that coagulation factor VIIa (FVIIa) elicits TF cytoplasmic domain-dependent proangiogenic cell signaling independent of the alternative PAR2 activator matriptase. We identify a Lys-Gly-Glu (KGE) integrin-binding motif in the FVIIa protease domain that is required for association of the TF-FVIIa complex with the active conformer of integrin β1. A point mutation in this motif markedly reduces TF-FVIIa association with integrins, attenuates integrin translocation into early endosomes, and reduces delayed mitogen-activated protein kinase phosphorylation required for the induction of proangiogenic cytokines. Pharmacologic or genetic blockade of the small GTPase ADP-ribosylation factor 6 (arf6) that regulates integrin trafficking increases availability of TF-FVIIa with procoagulant activity on the cell surface, while inhibiting TF-FVIIa signaling that leads to proangiogenic cytokine expression and tumor cell migration. These experiments delineate the structural basis for the crosstalk of the TF-FVIIa complex with integrin trafficking and suggest a crucial role for endosomal PAR2 signaling in pathways of tissue repair and tumor biology. (*Blood*. 2018;131(6):674-685)

Introduction

Tissue factor (TF) exerts dual functions as the initiator of coagulation and hemostasis and in directing cell signaling by TF-associated proteases that primarily cleave protease-activated receptor 1 or 2 (PAR1 or PAR2). Distinct pools of TF with different affinities for coagulation factor VIIa (FVIIa) support PAR signaling. Activation of PAR2 by TF-FVIIa is saturated only at relatively high FVIIa concentrations (~10 nM),[1-4] whereas activation of PAR1 or PAR2 by TF-FVIIa–generated nascent product FXa is already maximal at pM concentrations of FVIIa.[5-7] Signaling of the TF-FVIIa-FXa complex requires the endothelial protein C receptor (EPCR)[8] and is essential for induction of interferon-regulated genes downstream of innate immune toll-like receptor 4 signaling.[9] In contrast, signaling by TF-FVIIa can be inhibited by anti-TF antibody 10H10 which prevents association of TF with integrins, resulting in antitumor effects independent of blocking TF-dependent coagulation activation.[10] Although these data indicate that distinct receptor complexes support TF-dependent PAR signaling, a recent study proposed that upstream coagulation proteases initiate cell signaling indirectly through a common mechanism involving the PAR2 activator matriptase.[11,12] Thus, it remains incompletely understood how the TF-FVIIa complex signals by activating PAR2.

In addition to studies with monoclonal antibodies that implicate TF-dependent signaling in tumor progression and chronic inflammation,[10,13] direct inhibitors of TF-FVIIa have potent antiangiogenic properties in PAR2-dependent hypoxia-driven neovascularization[14,15] and attenuate colon cancer development.[16] Studies in an oncogene-driven mouse model of breast cancer have delineated a role for PAR2, but not PAR1, in promoting tumor development.[17] Tumor progression in this immune-competent model also requires the TF cytoplasmic domain[18] that is phosphorylated downstream of PAR2[19] and regulates integrins dependent on TF phosphorylation.[20-24] In addition to cancer cells that are known to ectopically synthesize upstream coagulation factors dependent on epigenetic mechanisms or hypoxia,[25-27] tumor-associated macrophages present another relevant source for FVII and FX in the tumor microenvironment.[28] Therefore, coagulation factors are present in extravascular locations, and it is important to understand the precise mechanism by which FVIIa elicits tumor cell PAR2 signaling and synthesis of a complex repertoire of immune modulatory and proangiogenic cytokines.[29]

The TF extracellular domain interacts with several heterodimers of integrin β1 as well as αvβ3.[20] Alternatively spliced TF retains the ability to ligate integrins αvβ3 and α6β1 for regulating endothelial function in angiogenesis, inflammation, and breast

cancer cell proliferation.[30-32] Although integrin ligation by alternatively spliced TF is independent of FVIIa, it is not well understood how FVIIa induces integrin effects in TF signaling. Here we identify the FVIIa integrin-binding motif that is required for complex formation of full-length TF with integrins. With a mutant defective in FVIIa-induced TF-integrin association, we demonstrate the functional importance of FVIIa in regulating TF-integrin β1 endocytosis during proangiogenic and promigratory signaling by the TF-FVIIa complex.

Methods

Materials

Recombinant human FVIIa wild-type (wt) and E26A mutant were produced at Novo Nordisk (Maløv, Denmark). PAR2 agonist peptide SLIGRL was synthesized in house.[33] The recombinant catalytic domain of human matriptase/ST14 was purchased from R&D Systems (Minneapolis, MN), MEK inhibitor U0126 from Cayman Chemicals (Ann Arbor, MI), PI3 kinase inhibitor LY290014 from Sigma-Aldrich (St. Louis, MO), arf6 modulator QS11 from Santa-Cruz Biotechnology (Santa Cruz, CA), and arf6 inhibitor SH3 from Tocris (Bristol, United Kingdom).

Adenoviral constructs

pcDNA3.1 constructs encoding for arf6 wt, T27N, or Q67L were kindly provided by Crislyn D'Souza-Schorey[34] and subcloned into pShuttle-cytomegalovirus. After recombination into AdEasy 1 vector, HEK 293 cells were used for adenovirus production as described for TF and PAR2-expressing adenoviruses.[5,19,21,35]

Cell culture

HaCaT keratinocytes[36] were grown in Dulbecco's modified Eagle medium (DMEM), 10% fetal calf serum, 1 mM glutamine, and 10 mM *N*-2-hydroxyethylpiperazine-*N*′-2-ethanesulfonic acid (HEPES). A7 melanoma cells[37] were transduced with human full-length TF or cytoplasmic domain–deleted TF (truncated after His243), PAR2, and where indicated, arf6 adenoviral expression vectors and cultured in Eagle's minimum essential medium (8% newborn calf serum, 2% fetal calf serum, 1 mM glutamine, 10 mM HEPES, 500 mg/L G418). MDA-MB-231mfp breast cancer cells and M24met melanoma cells were cultured as described previously.[10] Typically, cells were transferred 6 hours before stimulation into serum-free DMEM containing 1 mM glutamine and 10 mM HEPES.

Messenger RNA (mRNA) isolation and quantitative polymerase chain reaction

RNA was isolated with TRIzol Reagent (Life Technologies, Carlsbad, CA) and transcribed into complementary DNA using the SuperScript III First-Strand Synthesis System (Invitrogen, Life Technologies, Carlsbad, CA) for TaqMan quantitative polymerase chain reaction to quantify interleukin-8 (IL-8) with primers (Eurofins MWG Operon, Huntsville, AL) as described.[38]

Western blotting

We used the following antibodies: polyclonal anti-human TF antibody,[39] anti-human matriptase/ST14 catalytic domain antibody from R&D Systems (Minneapolis, MN), integrin β1 polyclonal antibody from Cell Signaling (Danvers, MA), and arf6 and HA-tag antibodies from Santa Cruz Biotechnology (Santa Cruz, CA). Cells were typically lysed in nonreducing sodium dodecyl sulfate sample buffer (Life Technologies) for gel electrophoresis.

Immunoprecipitation

After stimulation, cells were lysed in Brij 35 buffer (50 mM tris(hydroxymethyl)aminomethane (Tris)/HCl, 1% Brij 35, 150 mM NaCl, 1 mM $CaCl_2$, 1 mM $MgCl_2$ [pH 7.4] and freshly added protease and phosphatase inhibitors) for 15 minutes on ice. Cell lysates were cleared from debris, and the Brij 35–soluble fraction was separated from the insoluble fraction by centrifugation at 16 000*g* at 4°C for 30 minutes. Then, 0.5 mL of Brij 35–soluble fraction was incubated with antibodies conjugated to tosyl-activated paramagnetic DynaBeads M-450 (Life Technologies) at 4°C overnight. DynaBeads were rinsed 3 times with Brij 35 buffer, and bound proteins were eluted by adding 50 μL of nonreducing sodium dodecyl sulfate sample buffer at 90°C for 5 minutes.

Confocal microscopy

Cells were seeded on glass cover slips the day before and switched to serum-free medium for 6 hours before the experiment. In addition, 5 μg/mL fluorophore-labeled anti-FVIIa antibody 12C7 and anti-integrin β1 antibody TS2/16 produced in house were added to stimulations with FVIIa as indicated. Cells were fixed with 4% formaldehyde in phosphate-buffered saline for 10 minutes at room temperature and permeabilized with 0.1% Triton X-100. Alternatively, cells were incubated with FVIIa and fixed without permeabilization, followed by counterstaining with fluorophore-labeled anti-FVIIa antibody 3G12. For intracellular staining, surface FVIIa was blocked with unlabeled antibody, and fixed and permeabilized cells were then stained with labeled antibody. Intracellular targets were counterstained with anti–early endosome antigen 1 (EEA1) monoclonal antibody-Alexa Fluor 488 (MBL International, Woburn, MA), 5 μg/mL TS2/16-Alexa Fluor 488, and nuclei with 1 μg/mL Hoechst 33342 (Life Technologies). Cover slips were embedded in Fluorescent Mounting Medium (Dako, Carpinteria, CA) for imaging with a 63× or 40× oil emersion objective on a Zeiss 710 laser scanning microscope (Carl Zeiss, Jena, Germany). Images were processed by using ImageJ software (https://imagej.nih.gov/ij/).

Flow cytometry

Cells were recovered with trypsin/EDTA and stained with directly labeled antibodies to TF (5G9, 10H10) and integrin β1 (AIIB2) for flow cytometry.

Functional assay

Cells were rinsed once with HBS (10 mM HEPES [pH 7.4], 137 mM NaCl, 5.3 mM KCl, 1.5 mM $CaCl_2$). TF activity was determined by adding 0.5 mL HBS containing human FVIIa and 50 nM FX (Haematologic Technologies, Essex Junction, VT) to adherent cells per 12-well plate at 37°C. Activity of FXa was measured in 0.1M EDTA-quenched samples with the chromogenic substrate Spectrozyme FXa (Sekisui Diagnostics, Stamford, CT) by using a kinetic plate reader (Spectramax M2, Molecular Devices).

PAR2 cleavage

PAR2 cell surface cleavage was determined as previously described.[8,40] Briefly, Chinese hamster ovary cells were transfected to express FLAG-tagged PAR2. After incubation, uncleaved surface PAR2 was detected by using peroxidase-conjugated anti-FLAG antibody and 3,3′,5,5′-tetramethylbenzidine substrate, and the percentage of cleavage was calculated on the basis of unstimulated controls.

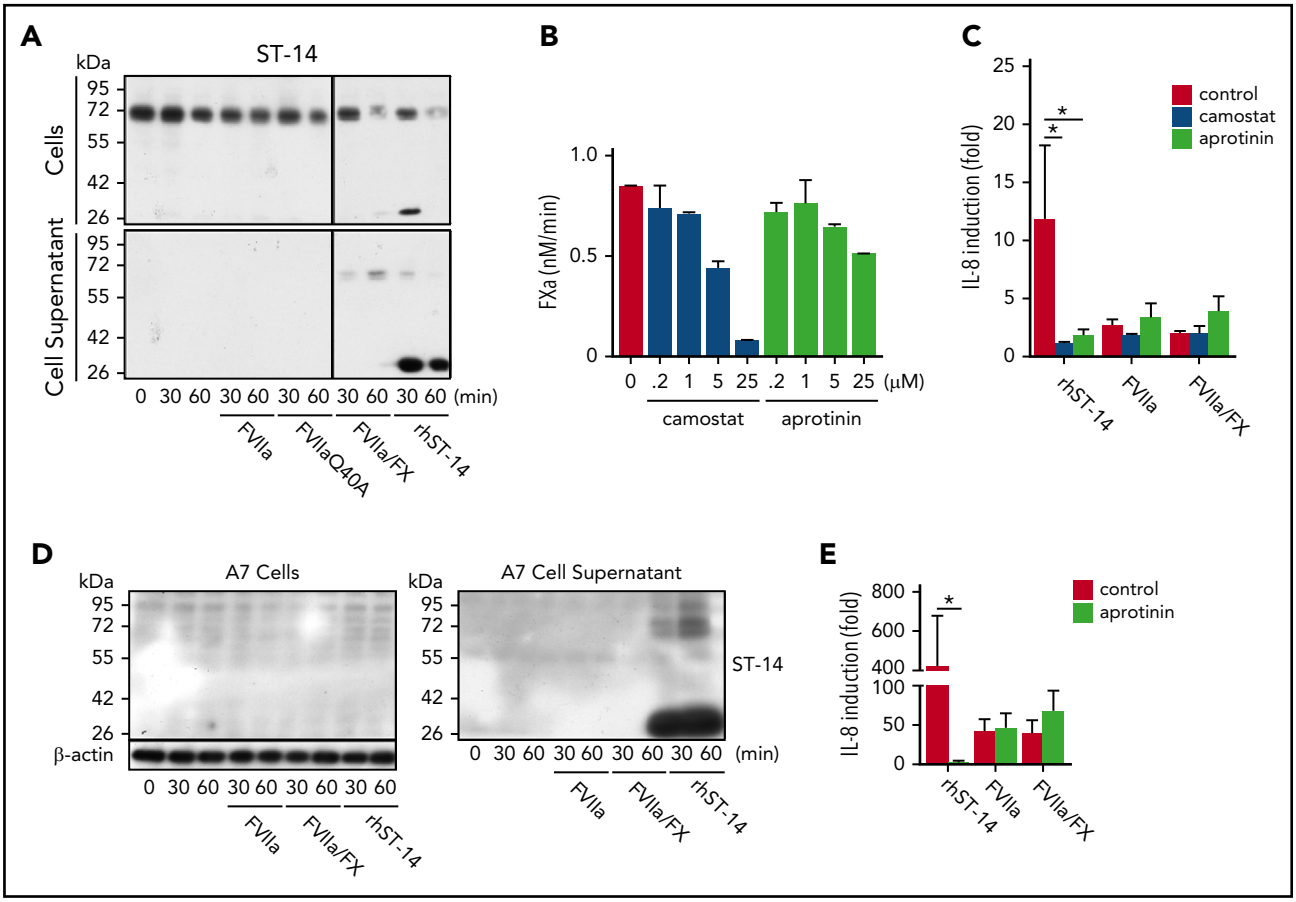

Figure 1. TF-FVIIa–induced IL-8 mRNA upregulation does not require matriptase activity. (A) Representative western blots of matriptase (ST-14) in cell lysates and cell-free supernatant from HaCaT cells stimulated with FVIIa (25 nM), signaling deficient FVIIa mutant Q40A (25 nM), FVIIa (1 nM)/FX (50 nM), and catalytic domain of recombinant human matriptase (rhST-14, 5 nM) for 30 and 60 minutes. Uncleaved matriptase has an apparent molecular weight of 72 kDa, whereas the protease domain is detected at 26 kDa. (B) HaCaT cell surface FXa generation with 10 nM FVIIa in the presence of indicated concentrations of protease inhibitors camostat and aprotinin. (C) IL-8 mRNA in HaCaT cells stimulated for 90 minutes with recombinant matriptase (rhST-14, 5 nM), FVIIa (10 nM), or FVIIa (1 nM)/FX (50 nM) in the absence or presence of serine protease inhibitors camostatin (1 μM) and aprotinin (5 μM) (n = 3; one-way analysis of variance (ANOVA) and Dunnett's test. (D) Representative western blot of matriptase (ST-14) in cells and cleared cell supernatant of A7 melanoma cells stimulated with FVIIa (25 nM), FVIIa (1 nM)/FX (50 nM), and recombinant human catalytic domain of matriptase (rhST-14, 5 nM) for 30 and 60 minutes, respectively. Because of their low inherent PAR2 signaling activity (PAR2 agonist SLIGRL induced IL-8 by 2.2- ± 1.0-fold, and FVIIa showed no induction of IL-8 [1.0- ± 0.3-fold]), A7 cells were transduced to express PAR2 and TF using adenoviral vectors. (E) Quantification of IL-8 mRNA in A7 melanoma cells stimulated for 90 minutes with recombinant matriptase (rhST-14, 5 nM), FVIIa (10 nM), or FVIIa (0.5 nM)/FX (50 nM) in the absence or presence of serine protease inhibitor aprotinin (5 μM) (n = 4). *$P < .05$, Student t test.

Migration assay

Migration assays were performed as described previously.[41] Briefly, migration of M24met human melanoma cells toward NIH3T3 fibroblast-conditioned medium was determined in Transwell chambers (Corning Incorporated, Kennebunk, ME). Cells were harvested from cell culture with a nonenzymatic method (Versene) to avoid PAR2 activation, stimulated for 30 minutes with FVIIa wt or mutant, and then added to the upper compartment of the migration chamber. Where indicated, cells were incubated with the arf6 inhibitor SH3 for 30 minutes before incubation with FVIIa. Cells were allowed to migrate for 4 hours and counted in the lower compartment of the migration chamber.

Results

TF-FVIIa–induced IL-8 mRNA upregulation does not require matriptase activity

Human keratinocyte (HaCaT) cells are an established model for studying TF-FVIIa signaling[3,5] and epithelial cell PAR2 activation by either the TF-FVIIa binary complex or the TF-FVIIa-Xa ternary complex, which can involve PAR2 cleavage by matriptase (ST-14) as an intermediary protease. Activation of membrane-bound matriptase results in the autocatalytic release of the catalytic domain. Consistent with a previous report,[11] we observed that stimulation with TF ternary complex facilitated matriptase release. However, at plasma concentrations, neither human FVIIa wt nor the signaling-deficient mutant FVIIa Q40A[40] promoted shedding of matriptase (Figure 1A).

Matriptase proteolytic activity and hence matriptase-induced PAR2 cleavage is blocked by protease inhibitors camostat and aprotinin.[11] We titrated the inhibitors in an FXa generation assay on HaCaT cells and determined that 5 μM aprotinin and 1 μM camostat did not interfere with TF-initiated coagulation (Figure 1B). At these concentrations, both inhibitors prevented IL-8 induction by exogenously added matriptase but had no effect on IL-8 upregulation by either the TF-FVIIa binary or the TF ternary complex (Figure 1C).

We previously used the TF-deficient A7 melanoma cell model to study TF interaction with integrin in cell migration and

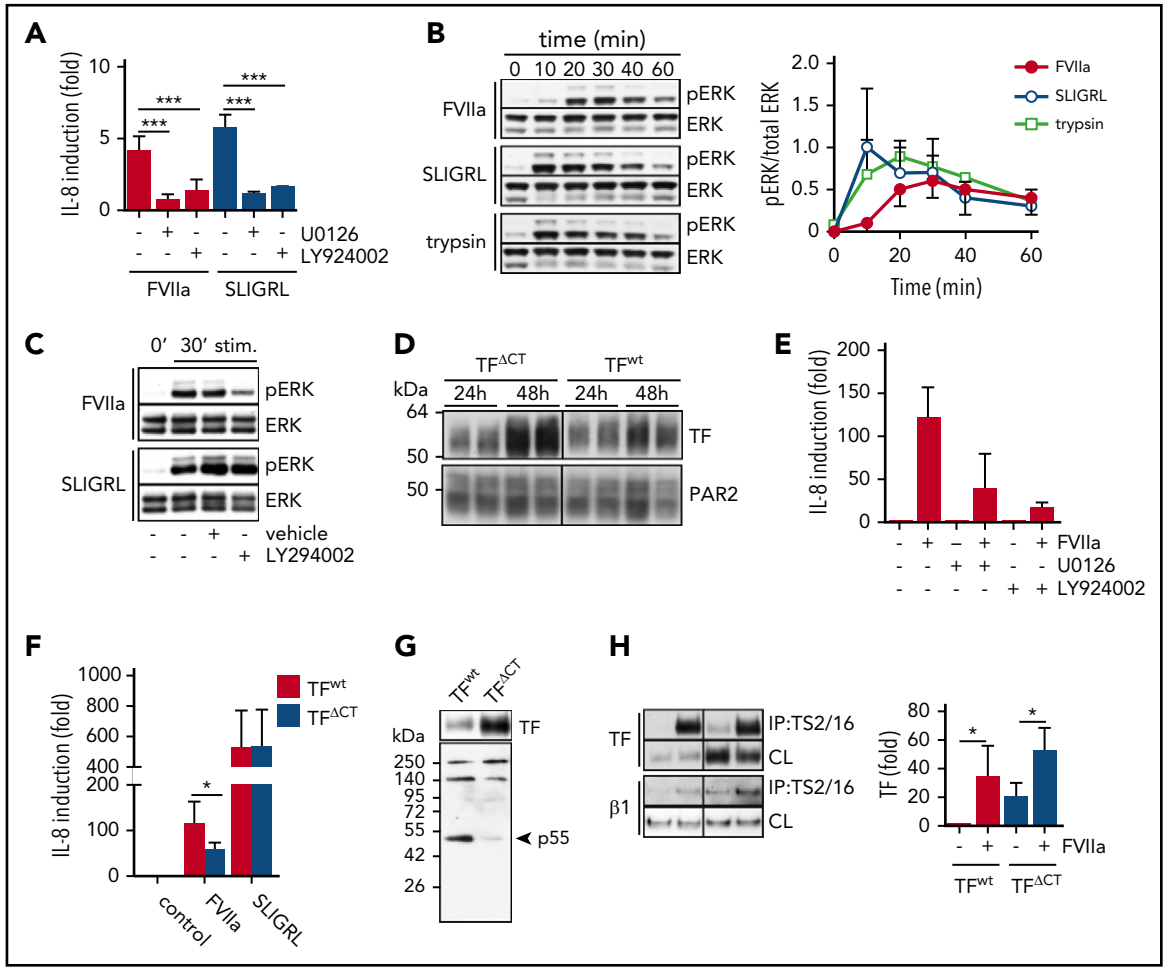

Figure 2. TF-FVIIa triggers a distinct PAR2 signaling pathway that involves PI3 kinase–dependent MAP kinase signaling. (A) IL-8 mRNA quantification of HaCaT cells stimulated with FVIIa (10 nM) and PAR2 agonist SLIGRL (50 μM) with or without MEK inhibitor U0126 (1 μM) and PI3K inhibitor LY294002 (1 μM) (n = 3-5). ***$P < .001$, one-way ANOVA and Dunnett's test. (B) Time course of ERK phosphorylation (pERK) in HaCaT cells stimulated with FVIIa (10 nM) or SLIGRL (50 μM). Upper panel: representative western blots of pERK and total ERK. Lower panel: densitometric quantification of pERK western blots from 3 independent experiments (n = 7). *$P < .05$, Student *t* test. (C) Western blots for pERK levels in HaCaT cells stimulated (stim) for 30 minutes with FVIIa (10 nM) and SLIGRL (50 μM) in the absence or presence of MEK inhibitor U0126 (1 μM) and PI3 kinase inhibitor LY294002 (1 μM). (D) Western blots of TF and PAR2 in A7 cells 24 and 48 hours after adenoviral transduction to express PAR2 as well as TF and TF$^{\Delta CT}$, respectively. (E) Quantification of IL-8 mRNA in A7 cells that were transduced to express TF wt and PAR2 48 hours before the experiment and stimulated with FVIIa (10 nM) for 90 minutes with and without MEK inhibitor U0126 (1 μM) or PI3 kinase inhibitor LY294002 (1 μM). (F) Quantification of IL-8 mRNA in A7 cells expressing full-length TF or TF$^{\Delta CT}$ stimulated for 90 minutes with FVIIa (10 nM) or SLIGRL (50 μM) (n = 3). *$P <$ .05, paired Student *t* test. (G) Western blot of TF and p55 in TF immunoprecipitates using αTF 5G9 antibody coupled to DynaBeads from A7 melanoma cells expressing full-length TF or TF$^{\Delta CT}$. (H) Representative western blots and densitometric quantification of 4 independent experiments of TF in a TS2/16 pull-down assay and cleared cell lysates from A7 cells expressing TF wt and TF$^{\Delta CT}$, respectively, after 30 minutes of stimulation with FVIIa (10 nM) (n = 4). *$P < .05$, one-way ANOVA and Tukey's test. CL, cleared-cell lysate; IP, immunoprecipitate.

TF-dependent metastasis.[20,42] Matriptase was not detected in western blots of cell lysates and cell supernatants of A7 melanoma cells, including after transduction with adenovirus to express TF and PAR2 (Figure 1D). Addition of recombinant matriptase induced IL-8 mRNA expression that was blocked by aprotinin; however, aprotinin did not inhibit TF-FVIIa–mediated upregulation of IL-8 induction (Figure 1E). Note that increased IL-8 induction was observed with both FVIIa and matriptase, indicating PAR2 overexpression in A7 relative to HaCaT cells. Thus, pharmacologic inhibitors and experiments in matriptase-deficient melanoma cells show that TF-FVIIa signaling induces proangiogenic cytokines independently of matriptase as a downstream intermediary.

TF-FVIIa triggers a distinct PAR2 signaling pathway that involves PI3 kinase-dependent MAP kinase signaling

FVIIa and PAR2 agonist SLIGRL induction of IL-8 in HaCaT cells was blocked by inhibitors of the mitogen-activated protein (MAP) kinase pathway (U0126) or PI3 kinase pathway (LY924002) (Figure 2A). However, FVIIa stimulation produced a distinct delay in MAP kinase ERK phosphorylation with a peak at 30 minutes, whereas ERK phosphorylation induced by the direct agonist SLIGRL or the soluble protease trypsin was already maximal after 10 minutes of stimulation (Figure 2B). In addition, although IL-8 induction by SLIGRL and FVIIa was sensitive to PI3 kinase inhibitor (Figure 2A), only FVIIa-induced ERK phosphorylation was dependent on PI3 kinase activity (Figure 2C).

Because the TF cytoplasmic domain is important for tumor progression in vivo,[18] we evaluated the contribution of the TF cytoplasmic domain to IL-8 induction in the A7 melanoma model. Virus doses were optimized for achieving similar expression of PAR2 along with full-length or cytoplasmic domain–deleted TF (TF$^{\Delta CT}$) documented at 24 hours after transduction (Figure 2D). Despite similar transduction efficiency, TF$^{\Delta CT}$ expression levels

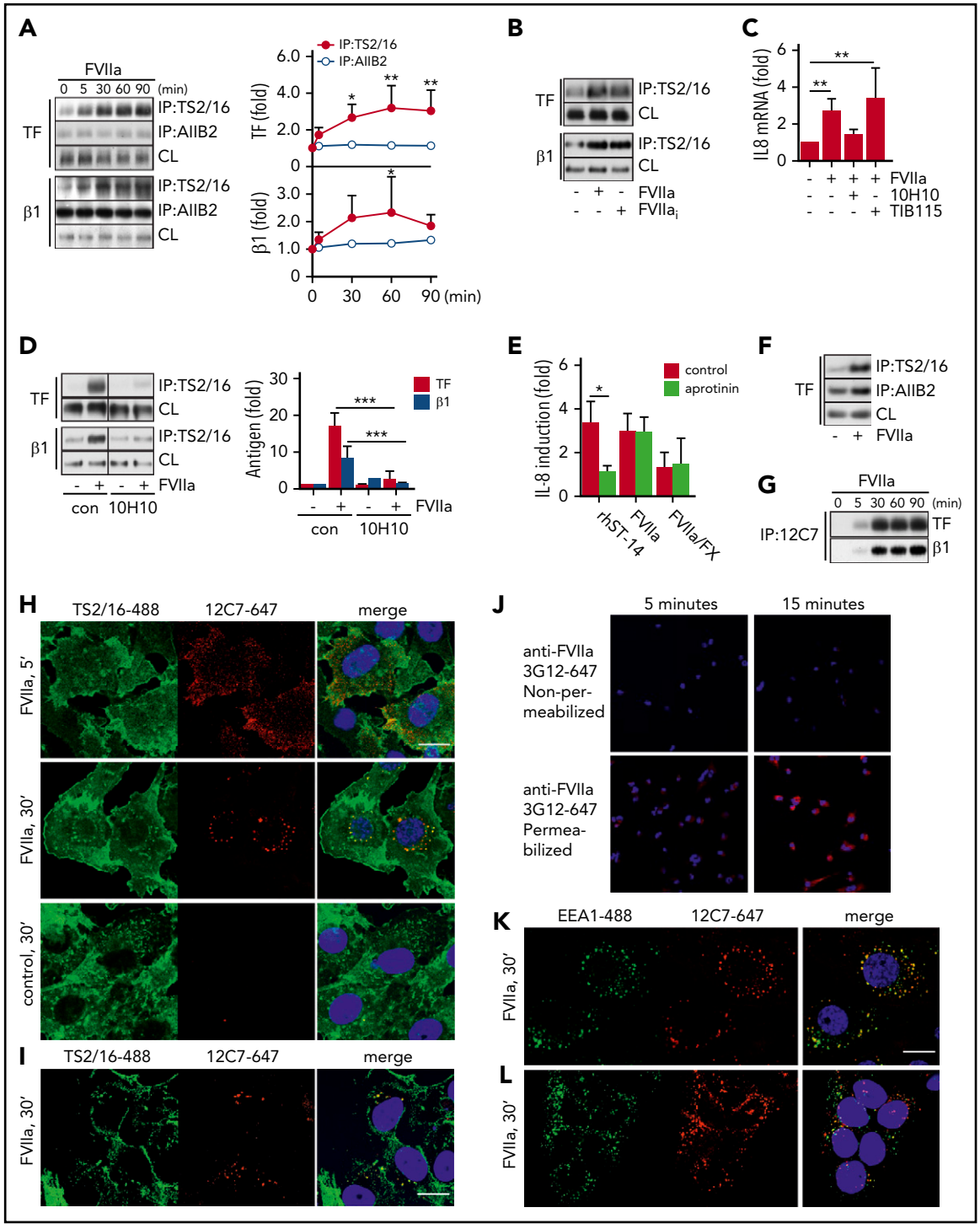

Figure 3. FVIIa promotes TF complex formation with the active conformer of integrin β1. (A) TF-integrin β1 interaction in HaCaT cells stimulated for indicated time points with FVIIa (10 nM). Left panel: representative western blots of TF and integrin β1 in immunoprecipitates from Brij 35 cell lysates using DynaBead-coupled integrin β1-specific antibodies TS2/16 (active conformer) or AIIB2. Right panel: densitometric quantification of western blots (n = 4). $^*P < .05$, $^{**}P < .01$, one-way ANOVA and Dunnett's test. (B) Representative western blot of TF and integrin β1 in a TS2/16 pull-down assay of Brij 35 lysates from HaCaT cells stimulated with FVIIa (10 nM) and active-site inhibited FVIIa$_i$ (10 nM) for 30 minutes. (C) Quantification of IL-8 mRNA in FVIIa-stimulated cells (10 nM) in the absence or presence of αTF antibody 10H10 (50 μg/mL) or control immunoglobulin G TIB115 (50 μg/mL) (n = 3). $^{**}P < .01$, one-way ANOVA and Dunnett's test. (D) FVIIa-induced TF-integrin β1 interaction in HaCaT cells incubated with or without 10H10 (50 μg/mL). Left panel: representative western blots of TF and integrin β1 in TS2/16 immunoprecipitates. Right panel: densitometric quantification of western blots (n = 4). $^{***}P < .01$, Student *t* test. (E) Quantification of IL-8 mRNA in MDA-MB-231 cells stimulated for 90 minutes with recombinant matriptase (rhST-14, 5 nM), FVIIa (10 nM), or FVIIa (0.5 nM)/FX (50 nM) in the absence or presence of serine protease inhibitor aprotinin (5 μM) (n = 3). $^*P < .05$, Student *t* test. (F) Representative western blot of TF in a TS2/16- and AIIB2 pull-down assay of Brij 35 lysates from MDA-MB-231 cells stimulated with FVIIa (10 nM) for 30 minutes. (G) Representative western blots of TF and integrin β1 in immunoprecipitates from Brij 35 cell lysates using DynaBead-coupled FVIIa-specific antibody 12C7. (H) For intracellular tracking of FVIIa, fluorophore-conjugate antibody anti-FVIIa 12C7-Alexa647 (5 μg/mL) was added to FVIIa stimulation (10 nM for indicated time) in MDA-MB-231 cells. After fixation, cells were counterstained for integrin β1 with TS2/16-fluorescein isothiocyanate (FITC) (5 μg/mL) and nuclei (Hoechst, 1 μg/mL). Scale bar = 10 μm. (I) Similarly, FVIIa was tracked in HaCaT cells over 30 minutes of stimulation by using fluorophore-conjugate antibody anti-FVIIa

continued to rise and were higher after 48 to 72 hours when this re-expression model reproduced the MAP kinase– and PI3 kinase–dependent induction of IL-8 (Figure 2E), as seen with HaCaT cells. Despite the higher expression of cytoplasmic domain–deleted TF, IL-8 induction by FVIIa was significantly reduced in A7 melanoma cells expressing $TF^{\Delta CT}$ compared with full-length TF (Figure 2F).

In addition, in TF pull-down assays, we found that the PI3 kinase regulatory subunit p55 co-immunoprecipitated specifically with full-length TF, but not $TF^{\Delta CT}$ (Figure 2G). These data indicate that the TF cytoplasmic domain directly recruits PI3 kinase required for proangiogenic TF-FVIIa signaling. Because the TF cytoplasmic domain regulates integrin function and cell migration,[20,22,23,43] we further evaluated whether previously demonstrated FVIIa-induced co-immunoprecipitation of TF with integrins[10] was dependent on the TF cytoplasmic domain. FVIIa induced a similar association of TF with integrins irrespective of the presence of the TF cytoplasmic domain (Figure 2H). Thus, the cytoplasmic domain of TF plays roles in IL-8 induction downstream of FVIIa-induced TF-integrin complex formation.

FVIIa promotes TF complex formation with the active conformer of integrin β1

With optimized immunoprecipitation from HaCaT cells, we found that FVIIa promoted TF association with integrin β1 immunoprecipitated with antibody TS2/16, which recognizes the active conformation of integrin β1.[44] Co-immunoprecipitation under these conditions was essentially undetectable with the inhibitory antibody AIIB2[44] (Figure 3A). In addition, FVIIa incubation for 30 minutes promoted a significant increase in immunoprecipitation of integrin β1 with TS2/16 that was independent of FVIIa catalytic activity (Figure 3B) and the TF cytoplasmic domain (Figure 2H), indicating that complex formation with TF-FVIIa induces recruitment of active integrin β1 into Brij 35–soluble membrane domains independent of TF-PAR2 signaling.

As previously shown,[10] anti-TF antibody 10H10, which has only moderate effects on cell surface FXa generation, blocked TF-FVIIa–induced IL-8 upregulation (Figure 3C) and FVIIa-mediated TF-integrin β1 complex formation detected in TS2/16 immunoprecipitates (Figure 3D). TF and PAR2 are required for tumor growth of MDA-MB-231mfp breast cancer cells,[10] which express similar levels of integrin β1 (HaCaT 2649 ± 713 mean fluorescence intensity [MFI]; MDA-MB-231mfp: 2809 ± 956 MFI) and twofold lower TF (HaCaT: 6195 ± 1774 MFI; MDA-MB-231mfp: 2467 ± 1268 MFI). IL-8 upregulation in response to FVIIa was also independent of matriptase activity (Figure 3E), and FVIIa promoted TF complex formation with the active conformer of integrin β1 (Figure 3F) in this pathophysiologically relevant tumor model.

To visualize the fate of FVIIa after cell binding, we used anti-FVIIa antibody 12C7 to an exosite epitope in the FVIIa protease domain.[45] Antibody 12C7 does not block the catalytic function, but it does interfere with binding and activation of macromolecular substrate FX. Antibody 12C7 did not inhibit TF-FVIIa induction of IL-8 (12C7: 2.6- ± 0.82-fold; control: 3.0- ± 0.84-fold induction) at the concentration (5μg/mL) used for imaging. In addition, antibody 12C7 immmunoprecipitated the TF-integrin β1 complex after addition of FVIIa to HaCaT cells (Figure 3G), confirming that it is noninhibitory.

AlexaFluor647-labeled anti-FVIIa antibody 12C7 was added to breast cancer cells stimulated with FVIIa, and after 5 or 30 minutes, cells were permeabilized for counterstaining with TS2/16 conjugated to AlexaFluor488 to visualize integrin β1. FVIIa was mainly present at the cell surface 5 minutes after addition but was found in perinuclear compartments after 30 minutes of stimulation (Figure 3H). No staining was seen in the absence of FVIIa, but FVIIa perinuclear staining was also detectable in HaCaT cells (Figure 3I). Importantly, FVIIa localized to organelles that also stained positive for integrin β1. Postfixation staining with fixation-insensitive anti-FVII antibody 3G12 after blocking cell surface FVIIa with unlabeled antibody confirmed that in permeabilized MDA-MB-231mfp, FVIIa was detectable intracellularly, excluding that internalization was dependent on the presence of the detecting antibody (Figure 3J). FVIIa staining co-localized with the early endosomal marker EEA1 in MDA-MB-231mfp (Figure 3K) and HaCaT cells (Figure 3L), but after 30 minutes of stimulation, no co-localization was observed with markers of lysosomes (Lamp-1), late endosomes (Rab7), and recycling endosomes (Rab11A) (data not shown). Because early endosomes serve as locations for MAP kinase signaling, the translocation of the TF-FVIIa-integrin complex into endosomes may be crucial for proangiogenic TF-FVIIa signaling.

The KGE integrin-binding motif in FVIIa is required for integrin β1 complex formation and proangiogenic cell signaling

Tripeptide motifs of a basic and acidic amino acid spaced by a neutral residue mediate integrin interaction. A Lys-Gly-Glu (KGE) motif, shown in the crystal structure of FVIIa (Figure 4A), is located within the macromolecular substrate binding exosite of the FVIIa protease domain.[45-47] A point mutation of glutamic acid 26 (E26) (chymotrypsin numbering) for alanine (FVIIa E26A) had only minimal effects on the cleavage of small chromogenic or macromolecular substrates (Figure 4B-C), indicating overall structural integrity of the FVIIa mutant. Moreover, cleavage assays[8] showed similar proteolytic cleavage of cell surface PAR2 by mutant or wt FVIIa (Figure 4D), demonstrating that the mutation does not affect the catalytic activity of FVIIa relevant for cell signaling.

However, FVIIa E26A was significantly impaired in inducing TF-integrin β1 complex formation (Figure 4E). The delayed ERK phosphorylation was attenuated when HaCaT cells were stimulated with FVIIa E26A compared with FVIIa wt (Figure 4F). Consistently, IL-8 upregulation was significantly reduced when cells were stimulated with FVIIa E26A (Figure 4G). Poor binding of 12C7 to FVIIa E26A limited the use of the antibody for intracellular tracking of the mutant, but prolonged incubation with FVIIa wt, but not FVIIa E26A, resulted in a significant downregulation of cell

Figure 3 (continued) 12C7-Alexa647 (5 μg/mL) and counterstaining for integrin β1 with TS2/16-FITC. Scale bar = 10 μm. (J) Postfixation staining of MDA-MB-231 cells after incubation with FVIIa for 5 and 15 minutes with anti-FVIIa 3G12-Alexa647 with and without permeabilization after blockade of surface FVIIa with unlabeled antibody. Confocal images of (K) MDA-MB-231 cells and (L) HaCaT cells incubated with anti-FVIIa 12C7-Alexa647 (5 μg/mL) during 30 minutes of stimulation with FVIIa (10 nM). Cells were counterstained for early endosomal marker EEA1 (αEEA1-Alexa488 conjugate, 5 μg/mL) and nuclei (Hoechst, 1 μg/mL) postfixation. Scale bar = 10 μm. con, control.

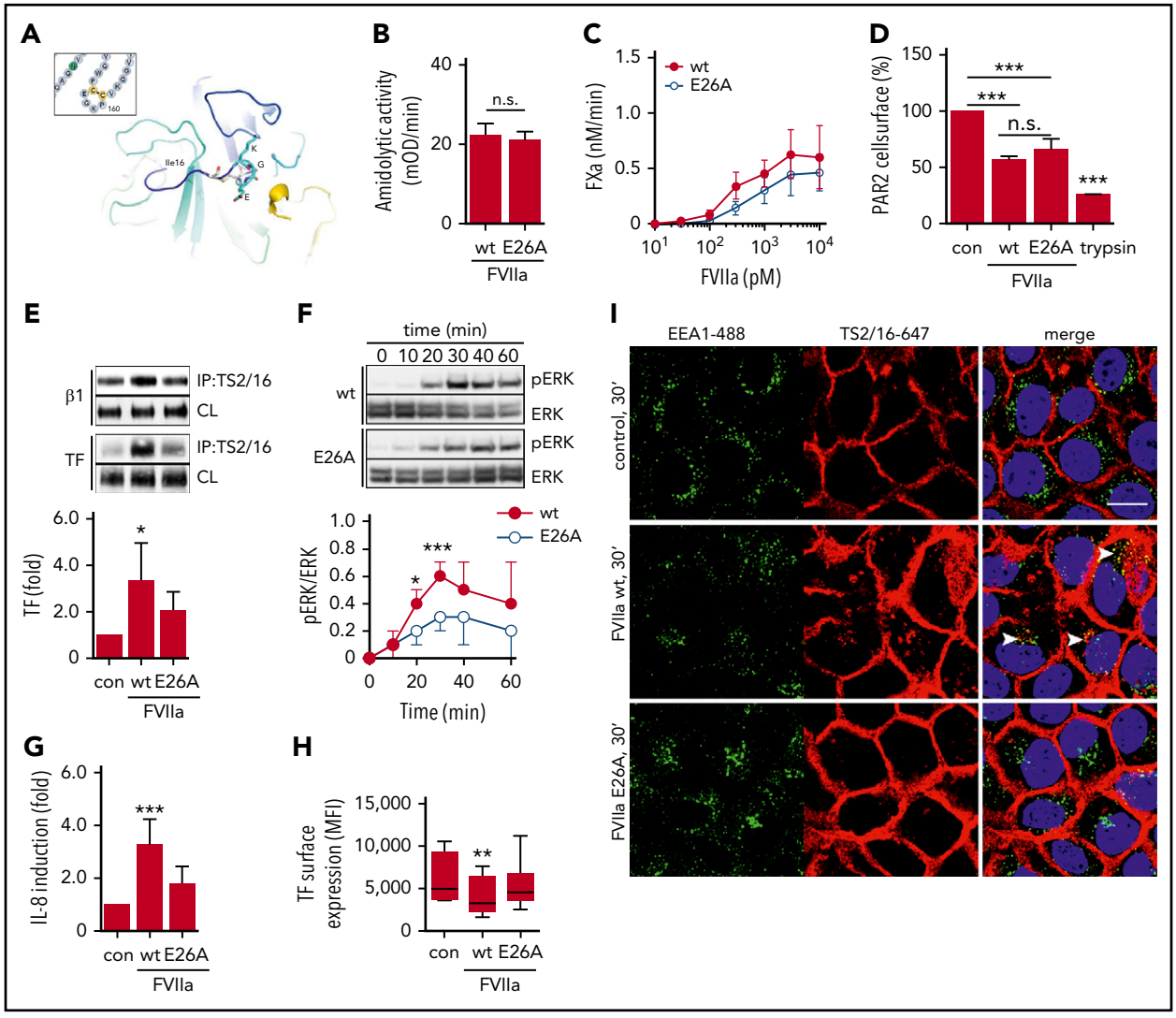

Figure 4. The KGE motif in FVIIa is required for integrin β1 complex formation and proangiogenic cell signaling. (A) Location of the surface-exposed KGE motif in the crystal structure of FVIIa.[68] (B) Amidolytic activity of FVIIa wt and E26A was measured by chromogenic substrate conversion (n = 4). $P = .503$, Student t test. (C) HaCaT cell-surface FXa generation with indicated concentrations of FVIIa E26A and FVIIa wt. (D) PAR2 receptor cleavage by FVIIa wt and E26A as well as trypsin in Chinese hamster ovary cells expressing FLAG-tagged PAR2 (n = 3). ***$P < .001$, one-way ANOVA and Dunnett's test. (E) TS2/16 immunoprecipitation of Brij 35 lysates from HaCaT cells stimulated with 10 nM FVIIa wt or E26A for 30 minutes. Upper panel: representative western blots of TF in TS2/16 immunoprecipitates and CLs. Lower panel: densitometric quantification of TF western blots (n = 6). *$P < .05$, one-way ANOVA and Dunnett's test. (F) Time course of ERK phosphorylation in HaCaT cells stimulated with 10 nM FVIIa wt or E26A. Upper panel: representative western blots of pERK and total ERK. Lower panel: densitometric quantification of pERK western blots normalized to total ERK of 3 independent experiments (n = 3). *$P < .05$, ***$P < .001$, Student t test. (G) Quantification of IL-8 mRNA in HaCaT cells stimulated for 90 minutes with 10 nM FVIIa wt and E26A, respectively (n = 8). ***$P < .001$, one-way ANOVA. (H) TF cell-surface expression of HaCaT cells stimulated with FVIIa wt and E26A determined by fluorescence-activated cell sorting (FACS) analysis (n = 7). **$P < .01$, one-way ANOVA. (I) Confocal imaging of HaCaT cells incubated with 10 nM FVIIa wt and E26A, respectively, in the presence of TS2/16-Alexa 647 conjugate (5 μg/mL). Cells were stained for early endosomes with αEEA1-Alexa488 (5 μg/mL) and nuclei (Hoechst, 1 μg/mL) after fixation. Scale bar = 10 μm. MFI, mean fluorescence intensity; n.s. not significant.

surface TF (Figure 4H). In addition, we found that surface-labeled integrin β1 detected by the active conformer antibody TS2/16 translocated to EEA1-positive compartments when cells were stimulated with FVIIa wt, but not with FVIIa E26A (Figure 4I). Taken together, these data show that the FVIIa KGE motif is required for TF-FVIIa complex formation with integrin β1 and integrin internalization, ERK phosphorylation, and IL-8 induction.

Arf6-dependent trafficking controls TF signaling and procoagulant function

We next evaluated whether integrin trafficking was important for TF-FVIIa signaling. Small GTPases control cell surface availability and internalization of integrins. In particular, arf6 control of integrin β1 has been shown to regulate cell signaling pathways relevant for cancer progression and angiogenesis.[48,49] In addition, we recently showed that arf6 regulated by integrin α4β1 in lipopolysaccharide-stimulated macrophages controls cell surface availability of TF for incorporation into microvesicles.[50] We used 2 small-molecule compounds to investigate the role of arf6-regulated integrin trafficking in cancer cell TF signaling. QS11 is a cell-permeable purine derivative that increases endogenous arf1- and arf6-guanosine triphosphate levels and hence increases arf6 activity, whereas secinH3 (SH3) inhibits the arf6-guanine nucleotide exchange factor cytohesin causing accumulation of nonactive arf6-guanosine diphosphate.[51,52] Cytohesin-1 inhibition with SH3 leads specifically to arf6, but not arf1, blockade.

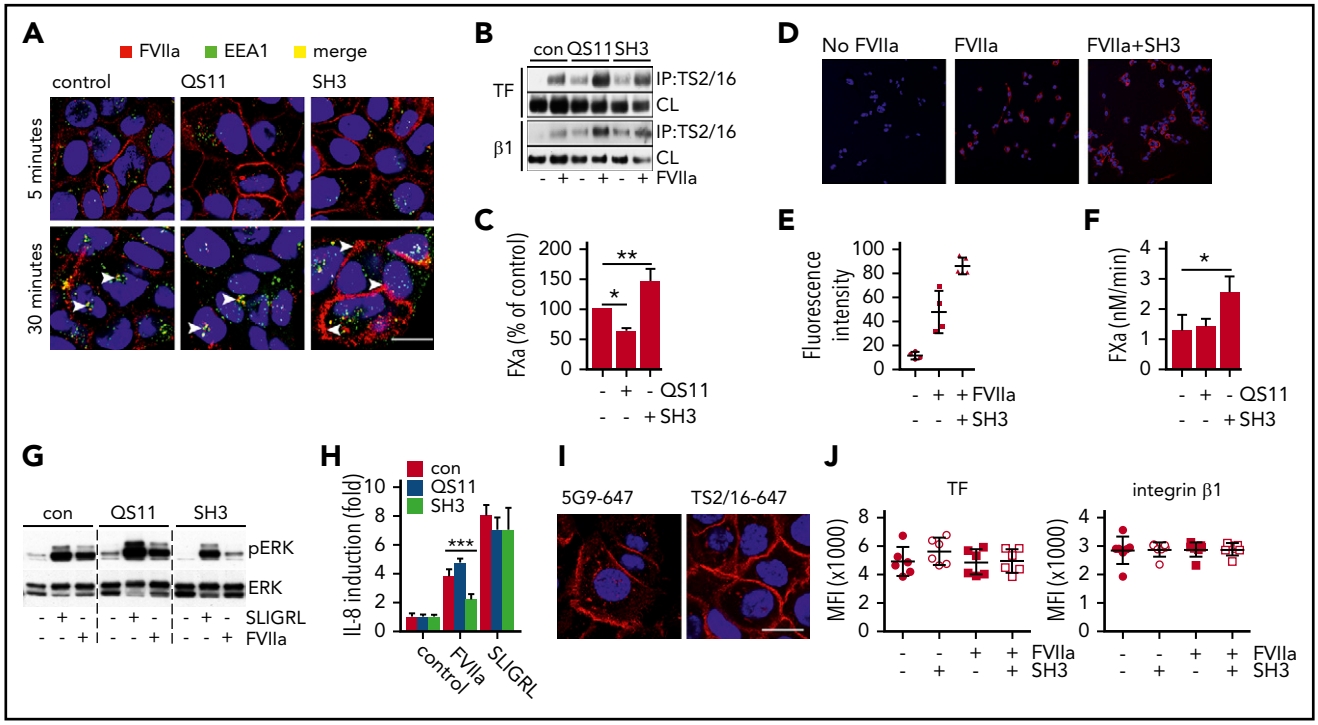

Figure 5. Arf6-dependent integrin recycling controls TF signaling and procoagulant function. HaCaT cells were pre-incubated with small-molecule inhibitors QS11 and SH3 for 2 hours. QS11 promotes arf6-GTP loading and thus it promotes arf6 activity, whereas SH3 inhibits arf6-GEF cytohesin, which causes accumulation of nonactive arf6-guanosine diphosphate. (A) Confocal imaging of HaCaT cells treated with QS11 (10 μM) or SH3 (20 μM). FVIIa (10 nM) was added together with FVIIa antibody 12C7-Alexa647 (red), and cells were incubated for 5 or 30 minutes. Upon fixation, cells were counterstained for early endosome antigen 1 (EEA1-Alexa488, green) and nuclei (Hoechst, blue). Scale bar = 10 μm. (B) TS2/16 immunoprecipitates and debris-cleared lysates (CLs) of Brij 35 cell lysates of HaCaT cells treated with QS11 (10 μM) and SH3 (20 μM) before FVIIa stimulation (10 nM; 30 minutes) were analyzed by western blot for TF and integrin β1. (C) FXa generation on HaCaT cells treated with QS11 and SH3 for 2 hours (n = 4). $*P < .05$, $**P < .01$, one-way ANOVA and Dunnett's test. (D) Representative surface staining for FVIIa after fixation with antibody 3G12 following exposure of MDA-MB-231 to FVIIa with or without SH3 pretreatment. (E) Quantification of fluorescent intensity of at least 4 random views from 2 independent experiments of cells treated as shown in panel D. Fluorescent intensity of images was quantified with imageJ software. (F) FXa generation on MDA-MB-231 cells as described in panel C. $*P < .05$. (G) ERK phosphorylation of HaCaT cells pretreated with arf6 inhibitors before stimulation with SLIGRL (50 μM) or FVIIa (10 nM) for 30 minutes. (H) Quantification of IL-8 mRNA induction in QS11- and SH3-pretreated HaCaT cells after 90 minutes of stimulation with SLIGRL (50 μM) or FVIIa (10 nM) (n = 4). $***P < .001$, one-way ANOVA and Tukey's test. (I) Representative confocal images of HaCaT cells stimulated with FVIIa (10 nM) for 30 minutes, fixed, permeabilized, and stained for TF (5G9-Alexa647) or integrin β1 (TS2/16-Alexa647). Scale bar = 10 μm. (J) FACS surface staining of TF and integrin β1 on HaCaT cells that were stimulated with FVIIa for 30 minutes (n = 7).

FVIIa detection after 5 minutes with fluorophore-labeled antibody 12C7 in HaCaT cells showed that FVIIa was similarly expressed on the cell surface irrespective of inhibitor pretreatment for 120 minutes. However, FVIIa appeared after 30 minutes of incubation in EEA1-positive early endosome in control and QS11-treated cells (Figure 5A). Although some residual cell surface FVIIa was detected in the control cells, FVIIa seemed to be more internalized in cells pretreated with arf6 stimulator QS11. In sharp contrast, incubation with the inhibitor SH3 prevented internalization and caused retention of FVIIa on the cell surface (Figure 5A). Pretreatment of HaCaT cells with these inhibitors did not impair FVIIa-induced co-immunoprecipitation of TF with integrin β1 (Figure 5B), confirming cell surface availability of the receptors. Consistent with the observed cell surface localization of FVIIa, TF-FVIIa–mediated FX activation was reduced in QS11-treated cells relative to control cells, but significantly increased after inhibition of arf6 with SH3 (Figure 5C). Similarly, cell surface localization of FVIIa determined by staining after fixation was significantly elevated in SH3-treated MDA-MB-231mfp cancer cells relative to control (Figure 5D-E), and SH3 increased FXa generation (Figure 5F).

Remarkably, despite increased cell surface availability of TF-FVIIa in HaCaT cells, SH3 prevented TF-FVIIa–mediated induction of ERK phosphorylation and of IL-8, supporting our hypothesis that intracellular trafficking to early endosomes is key for productive TF-FVIIa proangiogenic signaling (Figure 5G-H). Cell signaling induced by PAR2 agonist SLIGRL was not affected by pre-incubation with SH3 or QS11, demonstrating that inhibitors did not reduce PAR2 receptor availability and activity. Additional control experiments showed that after incubation with FVIIa for 30 minutes, abundant TF and integrin β1 remained on the cell surface and were detected by confocal microscopy (Figure 5I) or flow cytometry (Figure 5J), consistent with binding studies demonstrating that large pools of cell surface TF saturate slowly with FVIIa.[53] With blocking antibodies to EPCR, we also excluded that EPCR served as the receptor for FVIIa-induced IL-8 upregulation (anti-EPCR, 1496 3.6- ± 0.3-fold; control, 3.3- ± 1.2-fold induction over unstimulated cells). Thus, the integrin trafficking regulator arf6 controls cell surface availability and internalization of TF-FVIIa, and arf6 function is required for TF-FVIIa cell signaling activity.

We next investigated whether this pathway is also relevant in other tumor cells. Melanoma cells are known to depend on TF for metastasis[54] and primary tumor growth.[10] As seen with HaCaT keratinocytes, stimulation with FVIIa induced time-dependent complex formation of TF specifically with the active conformer of integrin β1 in A7 melanoma cells transduced with TF and PAR2 (Figure 6A), and FVIIa E26A showed markedly reduced induction of TF-integrin complex formation (Figure 6B) and consequently upregulation of IL-8 mRNA (Figure 6C).

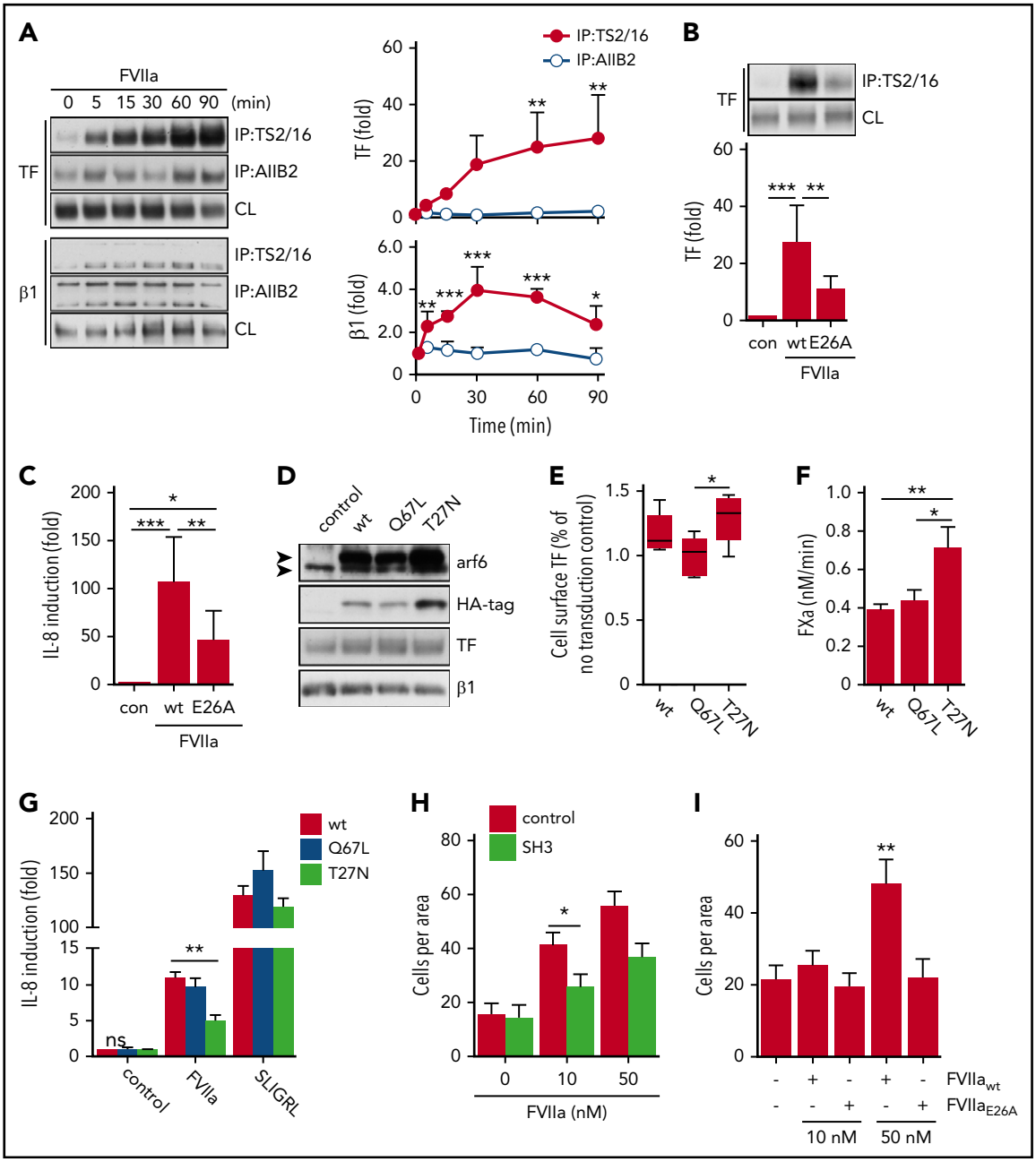

Figure 6. TF-FVIIa signaling in A7 melanoma cells requires FVIIa-mediated integrin complex formation and arf6 function. (A) TF-integrin β1 interaction in TF and PAR2 transduced A7 melanoma cells that were stimulated for indicated times with FVIIa (10 nM). Left panel: representative western blots of TF and integrin β1 in immunoprecipitates of Brij 35 cell lysates using DynaBead-coupled TS2/16 or AIIB2 antibody. Right panel: densitometric quantification of western blots (n = 4). $*P < .05$, $**P < .01$, $***P < .001$, one-way ANOVA and Dunnett's test. (B) Representative western blots and densitometric quantification of 4 independent experiments of TF in a TS2/16 pull-down assay from Brij 35 lysates from A7 cells stimulated with 10 nM FVIIa wt or E26A (n = 4). $**P < .01$, $***P < .001$. One-way ANOVA and Tukey's test. (C) Quantification of IL-8 mRNA in A7 cells after 90 minutes of stimulation with FVIIa wt (10 nM) or E26A (10 nM) (n = 7). $*P < .05$, $**P < .01$, $***P < .001$, ANOVA multiple comparison with Bonferroni correction. (D) Western blots of TF, integrin β1, arf6, and HA-tag of A7 cell lysates transduced to express HA-tagged arf6 wt, constitutively active mutant Q67L, or dominant-negative mutant T27N. (E) Cell surface expression of TF detected by antibody 5G9 in TF and PAR2 transduced cells co-expressing arf6 wt, Q67L, or T27N. Expression levels were normalized to TF and PAR2 transduced cells without arf6 virus from the same experiment (n = 5). $*P < .05$, one-way ANOVA and Tukey's test. (F) FXa generation on A7 cells expressing arf6 mutants (n = 3). $*P < .05$, $**P < .01$, one-way ANOVA and Dunnett's test. (G) IL-8 mRNA quantification in A7 cells expressing arf6 mutants after 90 minutes of stimulation with FVIIa (10 nM) or SLIGRL (50 μM) (n = 4). $**P < .01$, one-way ANOVA and Tukey's test. (H) Trans-well migration assay of highly motile M24met melanoma cells that were left untreated (black bars) or pre-incubated with SH3 (20 μM; white bars) before stimulation with 10 or 50 nM FVIIa (n = 3). $*P < .05$, Student *t* test. (I) Trans-well migration assay of M24met melanoma cells stimulated with 10 nM or 50 nM FVIIa wt and E26A (n = 3). $**P < .05$, one-way ANOVA and Tukey's test.

We next transduced A7 melanoma cells with TF, PAR2, and HA-tagged arf6 wt, constitutively active Q67L or dominant negative T27N[55] (Figure 6D). Overexpression of arf6 or mutants did not alter total levels of co-transduced TF or integrin β1 detected in cell lysates. However, cell surface TF expression detected by fluorescence-activated cell sorting was significantly higher in cells transduced with dominant negative arf6 T27N in comparison with constitutively active arf6 Q67L (Figure 6E). Consistent with data

obtained with pharmacologic inhibitors, dominant negative arf6 resulted in increased cell-surface TF-FVIIa activation of FX, pointing to reduced internalization of TF-FVIIa (Figure 6F). Conversely, FVIIa induction of IL-8 was significantly reduced in A7 cells expressing the dominant negative arf6 mutant relative to wt, whereas the direct PAR2 agonist SLIGRL induced IL-8 independent of arf6 activity (Figure 6G). Constitutively active arf6 was undistinguishable from wt in all assays, probably reflecting increased endogenous arf6 activity in cancer cells that are known to upregulate arf6 expression.[49,56]

TF-FVIIa signaling also stimulates cell migration of cancer and melanoma cells.[1,57] Additional studies with highly metastatic M24met melanoma cells with TF signaling-dependent tumor growth properties in vivo[10] showed that FVIIa-stimulated migration was reduced by the arf6 inhibitor SH3 (Figure 6H). In addition, only FVIIa wt, but not the integrin-binding defective mutant FVIIa E26A, stimulated melanoma cell migration (Figure 6I). Thus, integrin interaction and arf6-dependent trafficking to endosomal compartments are key events in TF-FVIIa proangiogenic and promigratory signaling.

Discussion

It is increasingly recognized that TF and its associated proteases assemble in multireceptor complexes (eg, with EPCR and integrins) to elicit cell-signaling events in innate immune defense,[9,58] angiogenesis,[14,59] vascular inflammation,[60] and cancer progression.[18,28] Optimal therapeutic targeting of these pleiotropic roles of the TF pathway requires an understanding of the underlying molecular and cellular mechanisms that determine TF signaling specificity. We previously showed that signaling of the TF-FVIIa binary complex can be selectively targeted with minimal effects on the hemostatic function of TF by interrupting the complex formation of TF with integrins.[10] In this study, we identified the molecular basis that governs the association of the TF-FVIIa complex with integrin β1 and demonstrated that this interaction is crucial for proangiogenic signaling of TF in keratinocytes and cancer cells.

We showed that FVIIa induces proangiogenic IL-8 induction independent of matriptase function or expression. FVIIa promotes an association of TF with integrin β1 that is preferentially immunoprecipitated by an antibody that recognizes the active conformation. Consistent with prior data demonstrating unaltered internalization in the absence of the TF cytoplasmic domain,[4,61] TF-FVIIa association with integrin β1 was independent of the TF cytoplasmic domain. The TF cytoplasmic domain was nevertheless required for proangiogenic IL-8 induction, consistent with in vivo evidence for a cooperation of PAR2 and TF cytoplasmic domain signaling in tumor- and obesity-promoting cell signaling.[13,18] Proangiogenic IL-8 induction was MAP kinase–, ERK-, and PI3 kinase–dependent, and TF coimmunoprecipitation of the regulatory subunit of PI3 kinase was abolished upon deletion of the TF cytoplasmic domain, which implicates this domain in the recruitment of PI3 kinase to the TF signaling complex. Although certain signaling events downstream of TF-FVIIa are independent of the TF cytoplasmic domain,[62,63] our data emphasize that tumor-promoting pathways of migration and proangiogenic cytokine induction[22,23,64,65] are critically dependent on the TF intracellular domain.

FVIIa induces the internalization of integrin β1 recognized by the activation-specific antibody TS2/16, which leads to colocalization of both proteins in endosomes. Mutation of the KGE integrin-binding site in FVIIa markedly diminished coimmunoprecipitation with TS2/16-recognized integrin β1, reduced integrin internalization, and attenuated proangiogenic IL-8 induction without measurable impairment of cell surface PAR2 cleavage. Unlike the peptide PAR2 agonist SLIGRL or the soluble protease trypsin, FVIIa promoted delayed ERK phosphorylation that was significantly reduced upon mutation of the FVIIa integrin-binding motif. Taken together, the data indicate that integrin association and endosomal translocation of TF-FVIIa triggers delayed ERK signaling that is required for the induction of proangiogenic cytokines.

TF-FVIIa internalization surprisingly also required the integrin-regulating small GTPase arf6.[66,67] Pharmacologic blockade of arf6 had no effect on FVIIa-induced TF association with integrins, which indicates unaltered physical interaction of the TF-FVIIa complex with integrin on the cell surface. However, pharmacologic arf6 inhibition or transfection with the dominant negative arf6 T27N substantially reduced proangiogenic IL-8 induction, while increasing cell surface availability of TF-FVIIa capable of activating the procoagulant substrate FX. Blockade of arf6 also attenuated FVIIa-induced cell migration that required the integrin-binding site of FVIIa. Taken together, our data identify the molecular basis for TF-FVIIa association with integrin and a crucial downstream signaling pathway that controls TF cell surface availability and internalization.

Acknowledgments

This work was supported by National Institutes of Health, National Heart, Lung, and Blood Institute grant HL60742 (W.R.), a fellowship from Novo Nordisk (A.S.R.), and the Alexander von Humboldt Foundation of Germany (W.R.).

Authorship

Contribution: A.S.R. designed, performed, and analyzed experiments and wrote the paper; E.L., S.C., and J.D. performed experiments; B.M.M. and H.Ø. analyzed data and provided critical reagents and input; and W.R. designed the study and wrote the paper.

Conflict-of-interest disclosure: The authors declare no competing financial interests.

Correspondence: Wolfram Ruf, Department of Immunology and Microbial Science, The Scripps Research Institute, 10550 North Torrey Pines Rd, La Jolla, CA 92037; e-mail: ruf@scripps.edu.

Footnotes

Submitted 9 February 2017; accepted 12 December 2017. Prepublished online as *Blood* First Edition paper, 15 December 2017; DOI 10.1182/blood-2017-02-768218.

The publication costs of this article were defrayed in part by page charge payment. Therefore, and solely to indicate this fact, this article is hereby marked "advertisement" in accordance with 18 USC section 1734.

REFERENCES

1. Hjortoe GM, Petersen LC, Albrektsen T, et al. Tissue factor-factor VIIa-specific up-regulation of IL-8 expression in MDA-MB-231 cells is mediated by PAR-2 and results in increased cell migration. *Blood*. 2004;103(8):3029-3037.

2. Versteeg HH, Hoedemaeker I, Diks SH, et al. Factor VIIa/tissue factor-induced signaling via activation of Src-like kinases, phosphatidylinositol 3-kinase, and Rac. *J Biol Chem*. 2000;275(37):28750-28756.

3. Camerer E, Gjernes E, Wiiger M, Pringle S, Prydz H. Binding of factor VIIa to tissue factor on keratinocytes induces gene expression. *J Biol Chem*. 2000;275(9):6580-6585.

4. Petersen LC, Albrektsen T, Hjortø GM, Kjalke M, Bjørn SE, Sørensen BB. Factor VIIa/tissue factor-dependent gene regulation and procoagulant activity: effect of factor VIIa concentration. *Thromb Haemost*. 2007;98(4):909-911.

5. Ahamed J, Versteeg HH, Kerver M, et al. Disulfide isomerization switches tissue factor from coagulation to cell signaling. *Proc Natl Acad Sci USA*. 2006;103(38):13932-13937.

6. Camerer E, Huang W, Coughlin SR. Tissue factor- and factor X-dependent activation of protease-activated receptor 2 by factor VIIa. *Proc Natl Acad Sci USA*. 2000;97(10):5255-5260.

7. Riewald M, Ruf W. Mechanistic coupling of protease signaling and initiation of coagulation by tissue factor. *Proc Natl Acad Sci USA*. 2001;98(14):7742-7747.

8. Disse J, Petersen HH, Larsen KS, et al. The endothelial protein C receptor supports tissue factor ternary coagulation initiation complex signaling through protease-activated receptors. *J Biol Chem*. 2011;286(7):5756-5767.

9. Liang HP, Kerschen EJ, Hernandez I, et al. EPCR-dependent PAR2 activation by the blood coagulation initiation complex regulates LPS-triggered interferon responses in mice. *Blood*. 2015;125(18):2845-2854.

10. Versteeg HH, Schaffner F, Kerver M, et al. Inhibition of tissue factor signaling suppresses tumor growth. *Blood*. 2008;111(1):190-199.

11. Le Gall SM, Szabo R, Lee M, et al. Matriptase activation connects tissue factor-dependent coagulation initiation to epithelial proteolysis and signaling. *Blood*. 2016;127(25):3260-3269.

12. Takeuchi T, Harris JL, Huang W, Yan KW, Coughlin SR, Craik CS. Cellular localization of membrane-type serine protease 1 and identification of protease-activated receptor-2 and single-chain urokinase-type plasminogen activator as substrates. *J Biol Chem*. 2000;275(34):26333-26342.

13. Badeanlou L, Furlan-Freguia C, Yang G, Ruf W, Samad F. Tissue factor-protease-activated receptor 2 signaling promotes diet-induced obesity and adipose inflammation. *Nat Med*. 2011;17(11):1490-1497.

14. Uusitalo-Jarvinen H, Kurokawa T, Mueller BM, Andrade-Gordon P, Friedlander M, Ruf W. Role of protease activated receptor 1 and 2 signaling in hypoxia-induced angiogenesis. *Arterioscler Thromb Vasc Biol*. 2007;27(6):1456-1462.

15. Hembrough TA, Swartz GM, Papathanassiu A, et al. Tissue factor/factor VIIa inhibitors block angiogenesis and tumor growth through a nonhemostatic mechanism. *Cancer Res*. 2003;63(11):2997-3000.

16. Zhao J, Aguilar G, Palencia S, Newton E, Abo A. rNAPc2 inhibits colorectal cancer in mice through tissue factor. *Clin Cancer Res*. 2009;15(1):208-216.

17. Versteeg HH, Schaffner F, Kerver M, et al. Protease-activated receptor (PAR) 2, but not PAR1, signaling promotes the development of mammary adenocarcinoma in polyoma middle T mice. *Cancer Res*. 2008;68(17):7219-7227.

18. Schaffner F, Versteeg HH, Schillert A, et al. Cooperation of tissue factor cytoplasmic domain and PAR2 signaling in breast cancer development. *Blood*. 2010;116(26):6106-6113.

19. Ahamed J, Ruf W. Protease-activated receptor 2-dependent phosphorylation of the tissue factor cytoplasmic domain. *J Biol Chem*. 2004;279(22):23038-23044.

20. Dorfleutner A, Hintermann E, Tarui T, Takada Y, Ruf W. Cross-talk of integrin alpha3beta1 and tissue factor in cell migration. *Mol Biol Cell*. 2004;15(10):4416-4425.

21. Dorfleutner A, Ruf W. Regulation of tissue factor cytoplasmic domain phosphorylation by palmitoylation. *Blood*. 2003;102(12):3998-4005.

22. Ott I, Fischer EG, Miyagi Y, Mueller BM, Ruf W. A role for tissue factor in cell adhesion and migration mediated by interaction with actin-binding protein 280. *J Cell Biol*. 1998;140(5):1241-1253.

23. Ott I, Weigand B, Michl R, et al. Tissue factor cytoplasmic domain stimulates migration by activation of the GTPase Rac1 and the mitogen-activated protein kinase p38. *Circulation*. 2005;111(3):349-355.

24. Ettelaie C, Elkeeb AM, Maraveyas A, Collier ME. p38α phosphorylates serine 258 within the cytoplasmic domain of tissue factor and prevents its incorporation into cell-derived microparticles. *Biochim Biophys Acta*. 2013;1833(3):613-621.

25. Koizume S, Jin MS, Miyagi E, et al. Activation of cancer cell migration and invasion by ectopic synthesis of coagulation factor VII. *Cancer Res*. 2006;66(19):9453-9460.

26. Koizume S, Yokota N, Miyagi E, et al. Hepatocyte nuclear factor-4-independent synthesis of coagulation factor VII in breast cancer cells and its inhibition by targeting selective histone acetyltransferases. *Mol Cancer Res*. 2009;7(12):1928-1936.

27. Koizume S, Ito S, Miyagi E, et al. HIF2α-Sp1 interaction mediates a deacetylation-dependent FVII-gene activation under hypoxic conditions in ovarian cancer cells. *Nucleic Acids Res*. 2012;40(12):5389-5401.

28. Schaffner F, Yokota N, Carneiro-Lobo T, et al. Endothelial protein C receptor function in murine and human breast cancer development. *PLoS One*. 2013;8(4):e61071.

29. Albrektsen T, Sørensen BB, Hjortø GM, Fleckner J, Rao LV, Petersen LC. Transcriptional program induced by factor VIIa-tissue factor, PAR1 and PAR2 in MDA-MB-231 cells. *J Thromb Haemost*. 2007;5(8):1588-1597.

30. Srinivasan R, Ozhegov E, van den Berg YW, et al. Splice variants of tissue factor promote monocyte-endothelial interactions by triggering the expression of cell adhesion molecules via integrin-mediated signaling. *J Thromb Haemost*. 2011;9(10):2087-2096.

31. van den Berg YW, van den Hengel LG, Myers HR, et al. Alternatively spliced tissue factor induces angiogenesis through integrin ligation. *Proc Natl Acad Sci USA*. 2009;106(46):19497-19502.

32. Kocatürk B, Van den Berg YW, Tieken C, et al. Alternatively spliced tissue factor promotes breast cancer growth in a β1 integrin-dependent manner. *Proc Natl Acad Sci USA*. 2013;110(28):11517-11522.

33. Ahamed J, Niessen F, Kurokawa T, et al. Regulation of macrophage procoagulant responses by the tissue factor cytoplasmic domain in endotoxemia. *Blood*. 2007;109(12):5251-5259.

34. Muralidharan-Chari V, Hoover H, Clancy J, et al. ADP-ribosylation factor 6 regulates tumorigenic and invasive properties in vivo. *Cancer Res*. 2009;69(6):2201-2209.

35. Ahamed J, Belting M, Ruf W. Regulation of tissue factor-induced signaling by endogenous and recombinant tissue factor pathway inhibitor 1. *Blood*. 2005;105(6):2384-2391.

36. Boukamp P, Petrussevska RT, Breitkreutz D, Hornung J, Markham A, Fusenig NE. Normal keratinization in a spontaneously immortalized aneuploid human keratinocyte cell line. *J Cell Biol*. 1988;106(3):761-771.

37. Cunningham CC, Gorlin JB, Kwiatkowski DJ, et al. Actin-binding protein requirement for cortical stability and efficient locomotion. *Science*. 1992;255(5042):325-327.

38. Carneiro-Lobo TC, Schaffner F, Disse J, et al. The tick-derived inhibitor Ixolaris prevents tissue factor signaling on tumor cells. *J Thromb Haemost*. 2012;10(9):1849-1858.

39. Sevinsky JR, Rao LVM, Ruf W. Ligand-induced protease receptor translocation into caveolae: a mechanism for regulating cell surface proteolysis of the tissue factor-dependent coagulation pathway. *J Cell Biol*. 1996;133(2):293-304.

40. Larsen KS, Ostergaard H, Olsen OH, Bjelke JR, Ruf W, Petersen LC. Engineering of substrate selectivity for tissue factor.factor VIIa complex signaling through protease-activated receptor 2. *J Biol Chem*. 2010;285(26):19959-19966.

41. Shi X, Gangadharan B, Brass LF, Ruf W, Mueller BM. Protease-activated receptors (PAR1 and PAR2) contribute to tumor cell motility and metastasis. *Mol Cancer Res*. 2004;2(7):395-402.

42. Gil-Bernabé AM, Ferjancic S, Tlalka M, et al. Recruitment of monocytes/macrophages by tissue factor-mediated coagulation is essential for metastatic cell survival and premetastatic niche establishment in mice. *Blood*. 2012;119(13):3164-3175.

43. Siegbahn A, Johnell M, Sorensen BB, Petersen LC, Heldin CH. Regulation of

chemotaxis by the cytoplasmic domain of tissue factor. *Thromb Haemost*. 2005;93(1):27-34.

44. Takada Y, Puzon W. Identification of a regulatory region of integrin beta 1 subunit using activating and inhibiting antibodies. *J Biol Chem*. 1993;268(23):17597-17601.

45. Dickinson CD, Shobe J, Ruf W. Influence of cofactor binding and active site occupancy on the conformation of the macromolecular substrate exosite of factor VIIa. *J Mol Biol*. 1998;277(4):959-971.

46. Shobe J, Dickinson CD, Ruf W. Regulation of the catalytic function of coagulation factor VIIa by a conformational linkage of surface residue Glu 154 to the active site. *Biochemistry*. 1999;38(9):2745-2751.

47. Norledge B, Petrovan RJ, Ruf W, Olson AJ. The tissue factor/factor VIIa/factor Xa complex: a model built by docking and site-directed mutagenesis. *Proteins*. 2003;53(3):640-648.

48. Caswell P, Norman J. Endocytic transport of integrins during cell migration and invasion. *Trends Cell Biol*. 2008;18(6):257-263.

49. Hongu T, Yamauchi Y, Funakoshi Y, Katagiri N, Ohbayashi N, Kanaho Y. Pathological functions of the small GTPase Arf6 in cancer progression: Tumor angiogenesis and metastasis. *Small GTPases*. 2016;7(2):47-53.

50. Rothmeier AS, Marchese P, Langer F, et al. Tissue factor prothrombotic activity is regulated by integrin-arf6 trafficking. *Arterioscler Thromb Vasc Biol*. 2017;37(7):1323-1331.

51. El Azreq MA, Garceau V, Harbour D, Pivot-Pajot C, Bourgoin SG. Cytohesin-1 regulates the Arf6-phospholipase D signaling axis in human neutrophils: impact on superoxide anion production and secretion. *J Immunol*. 2010;184(2):637-649.

52. Kanamarlapudi V, Thompson A, Kelly E, López Bernal A. ARF6 activated by the LHCG receptor through the cytohesin family of guanine nucleotide exchange factors mediates the receptor internalization and signaling. *J Biol Chem*. 2012;287(24):20443-20455.

53. Fair DS, MacDonald MJ. Cooperative interaction between factor VII and cell surface-expressed tissue factor. *J Biol Chem*. 1987;262(24):11692-11698.

54. Mueller BM, Reisfeld RA, Edgington TS, Ruf W. Expression of tissue factor by melanoma cells promotes efficient hematogenous metastasis. *Proc Natl Acad Sci USA*. 1992;89(24):11832-11836.

55. Palacios F, Price L, Schweitzer J, Collard JG, D'Souza-Schorey C. An essential role for ARF6-regulated membrane traffic in adherens junction turnover and epithelial cell migration. *EMBO J*. 2001;20(17):4973-4986.

56. Yamauchi Y, Miura Y, Kanaho Y. Machineries regulating the activity of the small GTPase Arf6 in cancer cells are potential targets for developing innovative anti-cancer drugs. *Adv Biol Regul*. 2017;63:115-121.

57. Morris DR, Ding Y, Ricks TK, Gullapalli A, Wolfe BL, Trejo J. Protease-activated receptor-2 is essential for factor VIIa and Xa-induced signaling, migration, and invasion of breast cancer cells. *Cancer Res*. 2006;66(1):307-314.

58. Antoniak S, Mackman N. Multiple roles of the coagulation protease cascade during virus infection. *Blood*. 2014;123(17):2605-2613.

59. Belting M, Dorrell MI, Sandgren S, et al. Regulation of angiogenesis by tissue factor cytoplasmic domain signaling. *Nat Med*. 2004;10(5):502-509.

60. Sparkenbaugh EM, Chantrathammachart P, Mickelson J, et al. Differential contribution of FXa and thrombin to vascular inflammation in a mouse model of sickle cell disease. *Blood*. 2014;123(11):1747-1756.

61. Hansen CB, Pyke C, Petersen LC, Rao LV. Tissue factor-mediated endocytosis, recycling, and degradation of factor VIIa by a clathrin-independent mechanism not requiring the cytoplasmic domain of tissue factor. *Blood*. 2001;97(6):1712-1720.

62. Sørensen BB, Freskgård PO, Nielsen LS, Rao LV, Ezban M, Petersen LC. Factor VIIa-induced p44/42 mitogen-activated protein kinase activation requires the proteolytic activity of factor VIIa and is independent of the tissue factor cytoplasmic domain. *J Biol Chem*. 1999;274(30):21349-21354.

63. Versteeg HH, Sørensen BB, Slofstra SH, et al. VIIa/tissue factor interaction results in a tissue factor cytoplasmic domain-independent activation of protein synthesis, p70, and p90 S6 kinase phosphorylation. *J Biol Chem*. 2002;277(30):27065-27072.

64. Siegbahn A, Johnell M, Rorsman C, Ezban M, Heldin CH, Rönnstrand L. Binding of factor VIIa to tissue factor on human fibroblasts leads to activation of phospholipase C and enhanced PDGF-BB-stimulated chemotaxis. *Blood*. 2000;96(10):3452-3458.

65. Siegbahn A, Johnell M, Nordin A, Aberg M, Velling T. TF/FVIIa transactivate PDGFRbeta to regulate PDGF-BB-induced chemotaxis in different cell types: involvement of Src and PLC. *Arterioscler Thromb Vasc Biol*. 2008;28(1):135-141.

66. D'Souza-Schorey C, Chavrier P. ARF proteins: roles in membrane traffic and beyond. *Nat Rev Mol Cell Biol*. 2006;7(5):347-358.

67. Nishiya N, Kiosses WB, Han J, Ginsberg MH. An alpha4 integrin-paxillin-Arf-GAP complex restricts Rac activation to the leading edge of migrating cells. *Nat Cell Biol*. 2005;7(4):343-352.

68. Banner DW, D'Arcy A, Chène C, et al. The crystal structure of the complex of blood coagulation factor VIIa with soluble tissue factor. *Nature*. 1996;380(6569):41-46.